Quantifying Atmospheric Trace Element Deposition over the Ocean on a Global Scale with Satellite rainfall products

David Kadko[1], William Landing[2], Clifton Buck[3]

[1] Florida International University, Applied Research Center, Miami, FL, USA
[2] Department of Earth, Ocean and Atmospheric Science, Florida State University, Tallahassee, FL, USA
[3] Skidaway Institute of Oceanography, University of Georgia, Savannah, GA, USA

Corresponding author: David Kadko (dkadko@fiu.edu)

Key Points:

1. Aerosol input of trace element micronutrients is difficult to determine as aerosol chemical concentration alone cannot yield deposition rate

2. The natural radionuclide ^{7}Be provides a means to estimate the bulk deposition velocity (V_b) required for this calculation

3. We use new ^{7}Be data from the Pacific with data from other ocean basins to derive a global relationship between rain rate and V_b

Key words

Trace elements, GEOTRACES, aerosols, bulk deposition velocity

Abstract

Atmospheric input of trace element micronutrients to the oceans is difficult to determine as even with collection of high-quality aerosol chemical concentrations such data by themselves cannot yield deposition rates. To transform these concentrations into rates, a method of determining flux by applying an appropriate deposition velocity is required. A recently developed method based on the natural radionuclide ^{7}Be has provided a means to estimate the bulk (wet + dry) deposition velocity (V_b) required for this calculation. Here, water column ^{7}Be inventories and aerosol ^{7}Be concentrations collected during the 2018 US GEOTRACES Pacific Meridional Transect are presented. We use these data together with those from other ocean basins to derive a global relationship between rain rate (m/y) and bulk depositional velocity (m/d), such that V_b = 999±96 x Rain rate + 1040±136 (R^2=0.81). Thus with satellite -derived rainfall estimates, a means to calculate aerosol bulk deposition velocities is provided.

Plain Language Summary

Atmospheric input of trace element micronutrients to the global ocean such as iron (Fe), cobalt (Co) and Zinc (Zn) is difficult to determine. Even with collection of high-quality aerosol chemical concentrations such data by themselves cannot yield rates of deposition. A recently developed method based on the natural radionuclide ^{7}Be which is deposited to the surface ocean has provided a means to estimate the bulk (wet + dry) deposition velocity (V_b) required for this calculation. In this work, water column ^{7}Be inventories and aerosol ^{7}Be concentrations collected during the 2018 US GEOTRACES Pacific Meridional Transect are presented. We use these data together with those from other ocean basins to derive a global relationship between rain rate (m/y) and bulk depositional velocity (m/d), such that V_b = 999xRain rate + 1040 (R2=0.81). Thus given a global rain product, a means to estimate deposition velocities based on rainfall is provided. This information is a critical for evaluating limitations on phytoplankton growth and the strength of the Biological Carbon Pump, and represents an important input to ocean biogeochemical models.

1. INTRODUCTION

As the base of most marine food webs, phytoplankton productivity affects growth and success at all other trophic levels in the oceans. Phytoplankton growth rates are controlled in part by macro and micronutrient supply rates, which in turn are controlled by physical environmental factors (atmospheric deposition, vertical mixing, upwelling, and horizontal advection) which vary over (and often define) different oceanic regimes. The magnitude of these fluxes will therefore vary significantly across ocean basins (e.g. Buck et al., 2019; Kadko et al., submitted). The Biological Carbon Pump (BCP), one of the

dominant mechanisms for sequestering atmospheric carbon to the deep ocean (Volk and Hoffert, 1985), is related to the interplay between different limiting factors such as the concentrations of available macronutrients (silicon, Si; phosphorus, P; nitrogen, N) and essential micronutrients like manganese (Mn), iron (Fe), cobalt (Co), nickel (Ni), copper (Cu), zinc (Zn), and cadmium (Cd). Understanding the factors that control the sources and distributions of bioactive trace elements (TEs) is crucial for predicting their effects on the BCP.

Atmospheric input to the oceans can be significant for many chemical species (e.g., Duce et al., 1991; Prospero, 1996, 2002). TE micronutrients delivered to the open ocean by dust deposition may, in some areas, relieve TE limitation on phytoplankton growth and promote nitrogen fixation (e.g. Martin et al., 1990, Coale et al., 1996; Falkowski, 1997; Falkowski et al., 1998; Moore et al., 2009; 2013; Krishnamurthy et al., 2009; Jickells et al., 2014; Baker and Jickells, 2016; Okin et al. 2011) and can play an important role in controlling biogeochemical processes in the ocean (e.g. Morel et al., 2003; Morel and Price, 2003). For these reasons, considerable effort has been made to evaluate the supply of dust to the ocean (e.g. Anderson et al., 2016; Baker et al., 2016) including consideration of dust supply in global biogeochemical models (e.g. Mahowald et al., 2005; Tagliabue et al., 2009; 2015).

Despite these efforts, the determination of the dust flux, particularly in remote ocean regions, is difficult (Anderson et al., 2016; Baker et al., 2016). While direct collection of atmospheric aerosols is relatively straightforward there is limited availability of island sampling locations and limited time that aerosols can be collected during a research cruise. Furthermore, even with high-quality aerosol chemical concentrations obtained from shipboard or land-based aerosol samples, such concentration data by themselves cannot yield the deposition rate of TEs. To transform these concentrations into rates, a method of determining flux by applying an appropriate deposition velocity is required. Similarly, models may be inaccurately configured (or "poorly constrained") regarding the parameterization of atmospheric deposition processes. If such parameters could be accurately assessed, then the chemical concentrations in aerosol samples could be converted into actual estimates of flux.

A recently developed method based on the natural radionuclide ^{7}Be (half-life 53.3 days), has shown promise as a way to estimate atmospheric deposition fluxes (Kadko et al., 2015). This method has been used to derive TE atmospheric fluxes for sites in the Atlantic (Kadko et al., 2015; Anderson et al., 2016; Shelley et al., 2017), the Pacific (Buck et al., 2019; Kadko et al., submitted) and the Arctic (Kadko et al., 2016; 2019; Marsay et al., 2018) oceans. ^{7}Be is produced in the upper atmosphere from cosmic ray spallation, quickly attaches to aerosol particles, and is transported to the lower troposphere by atmospheric mixing processes and removed mainly by precipitation. In this work, water column ^{7}Be inventories and aerosol ^{7}Be concentrations collected during the 2018 US GEOTRACES Pacific Meridional Transect (PMT; GEOTRACES section GP15) are presented. We use these data together with

data from other ocean basins to derive a global relationship between rain rate and aerosol bulk deposition velocity. Thus given a global rain product, a means to estimate deposition velocities based on rainfall is provided.

2. Background

The bulk flux for aerosol TEs (F_{TE}) is estimated from the concentration of trace elements in aerosols (C_{TE}) and the bulk deposition velocity (V_b) which includes dry + wet deposition, such that

$$F_{TE} = V_b \times C_{TE} \qquad \text{Eqn. 1}$$

Based on ^{7}Be, V_b can be derived from:

$$V_b = \frac{[\,^{7}Be \text{ flux }]}{(^{7}Be)_{aerosol}} \qquad \text{Eqn. 2}$$

Furthermore, it has been shown that the integrated rate of decay of ^{7}Be in the upper ocean (i.e. the ^{7}Be inventory in the water column multiplied by the radioactive decay constant for ^{7}Be) is equal to its flux to the ocean by wet and dry deposition (Aaboe et al., 1981; Kadko and Prospero, 2011; Kadko et al., 2015; Kadko et al., 2019) under steady-state conditions, such that:

$$V_b = (\text{Inventory } ^{7}Be \times \lambda) / (^{7}Be)_{aerosol} \qquad \text{Eqn. 3}$$

where λ is the ^{7}Be decay constant (0.013 d^{-1}). This observation provides a key linkage between the atmospheric concentrations of chemical species and their deposition to the oceans; the flux from the atmosphere to the surface ocean of any material having a deposition velocity similar to that of ^{7}Be can be calculated from its atmospheric concentration and the ^{7}Be-derived bulk deposition velocity (Young and Silker, 1980).

This method was tested at the BATS (Bermuda Atlantic Time Series) site in the Sargasso Sea (Kadko et al., 2015), where TE fluxes based on the ^{7}Be method were compared with 24 months of continuous aerosol and rainfall sampling at the BIOS (Bermuda Institute of Ocean Sciences) station on Bermuda. The atmospheric fluxes of total aerosol TEs (Fe, Mn, Co, Ni, Cu, Zn, Cd, and Pb), calculated using the bulk deposition velocity determined from the ^{7}Be data, were comparable (50% to 95%) to fluxes derived from measured wet deposition plus estimated dry deposition (assuming V_d = 1000m/day) for samples collected on Bermuda. This method was also tested during the 2015 US Arctic GEOTRACES cruise by comparing ^{7}Be-derived TE fluxes to the measured TE accumulation in recently deposited snow.

Given the variability in snow and aerosol TE concentration observed over the expedition, and the limited timescale of the observations, agreement between the two methods was reasonable.

Because it is associated with sub-micrometer aerosols, the deposition of aerosol ^{7}Be is dominated by rainfall scavenging, and it has been observed that ^{7}Be deposition rates correlate with the rate of precipitation (e.g. Young and Silker, 1980; Olsen et al., 1985; Uematsu et al., 1994; Kim et al., 1999; Kadko and Prospero, 2011; Peng et al., 2019). The ^{7}Be-derived bulk deposition velocity from the Arctic (low rainfall region) was 1190 m/d (Kadko et al 2016; 2019) and from Bermuda (high rainfall region) was 2600 m/d (Kadko et al., 2015). These are plotted against rain-fall rate in Supplemental Figure 1. Obviously, a trend cannot be based on only two points, but the zero-rainfall intercept does correspond to the dry deposition velocity of 1000 m/d generally assumed for dust (e.g. Duce et al., 1991). These results are suggestive of a relationship between V_b and rain rate that will be further explored here.

3. Study area and Methods

The US GEOTRACES Pacific Meridional Transect (PMT, cruise GP15) was carried out on the R/V Roger Revelle from September 25 to November 25, 2018. The cruise mainly followed a north-to-south track along 152° W between Alaska and Tahiti (Figure 1), designed to examine, among other things, the influence of strong margin chemical fluxes, atmospheric dust deposition, oxygen minimum zones, equatorial upwelling, and some of the lowest-nutrient waters in the world ocean in the South Pacific gyre at 20°S. This transect crossed large gradients in rain rate (Figure 1) affording an opportunity to test the V_b and rain rate relationship.

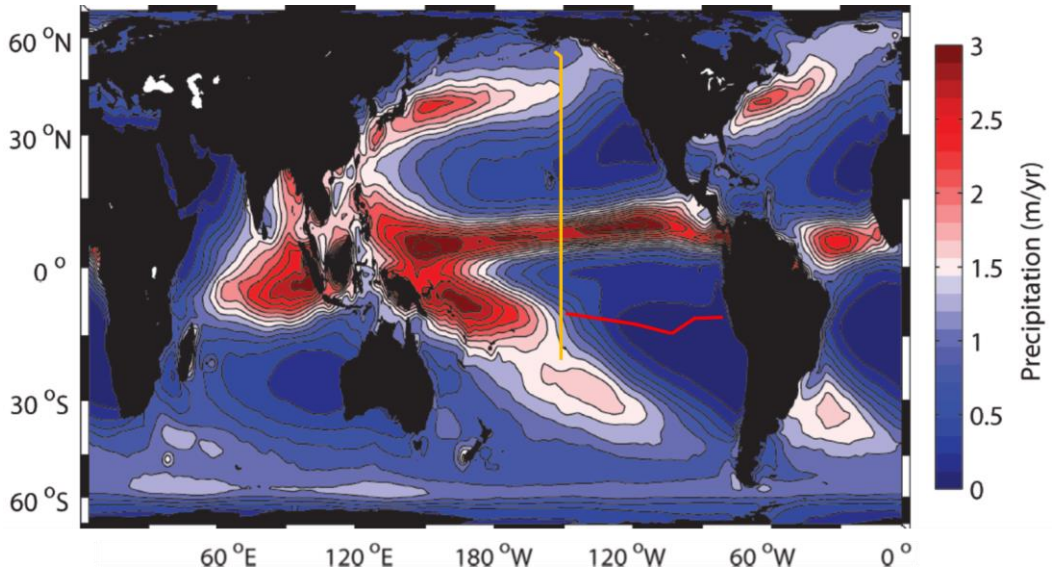

Figure 1. The track (yellow line) of the 2018 GEOTRACES PMT (GP15) cruise superimposed over a climatological map of precipitation, from Schanze et al. (2010). Also shown is the track (red line) of the 2013 GEOTRACES GP16 (East Pacific Zonal Transect; Kadko et al., submitted)

3.1. ^{7}Be water column analysis: Details of sample collection are described in Kadko (2017). Briefly, samples were collected at selected depths by pumping 400–700 L of seawater via a ~4 cm hose into large plastic barrels on deck. From these barrels, the seawater was then pumped through iron impregnated acrylic fibers at ~10 L/min to extract the ^{7}Be from seawater (Lal et al., 1988; Krishnaswami et al., 1972; Lee et al., 1991). On land, the fibers were dried and then ashed. The ash was subsequently pressed into a pellet (5.8 cm diameter) and placed on a low background germanium gamma detector. The isotope ^{7}Be has a readily identifiable gamma peak at 478 keV. The detector was calibrated for the pellet geometry by adding a commercially prepared mixed solution of known gamma activities to an ashed fiber, pressing the ash into a pellet, and counting the activities to derive a calibration curve. The uncertainty of the extraction efficiency (4%) and the detector efficiency (2%) was in all cases smaller than the statistical counting error and the uncertainty in the blank.

3.2. Aerosol ^{7}Be: Details of the aerosol collection methods are presented in Buck et al., (2019). Briefly, bulk aerosol samples were collected on 12-replicate acid-washed 47 mm Whatman 41(W41) ash-less filter discs mounted in Advantec-MFS polypropylene inline filter holders (PP47). When the wind was directed from the bow, air was pumped through the filters using a high-volume aerosol sampler (model 5170V-BL, Tisch Environmental) at approximately 100 L min^{-1} through each filter. The sampler was mounted on the forward rail of the 03-deck approximately 16 m above sea level and forward of both the ship's superstructure and exhaust stacks. Each collection period lasted approximately three days. For ^{7}Be, Whatman-41 aerosol filters were stacked three-high in a plastic Petri dish and counted by gamma spectroscopy. This configuration was calibrated with a commercially prepared mixed solution of known gamma activities.

3.3. Rainfall analysis. Rainfall data was derived from the Global Precipitation Climatology Project (GPCP). The GPCP monthly product provides a consistent analysis of global precipitation from an integration of various satellite data sets over land and ocean and gauge data from land sites http://gpcp.umd.edu/. The rainfall rates used in the following discussions were based on the weighted average at each location which included the rain rate for the month of sampling, and the prior three months each diminished by an exponential term containing the decay constant of ^{7}Be; that is, weighted against the decay lifetime of ^{7}Be deposited during each month.

$$\text{Average rain rate} = \Sigma\, RR_i \cdot f_i \exp(-\lambda t_i) / \Sigma\, f_i \exp(-\lambda t_i) \qquad \text{Eqn. 4}$$

where RR_i is the rainfall rate for month (i) taken from the GPCP data set, f_i ($0 \leq f_i \leq 1$) is the fraction of the month during the month of sampling (e.g. November 15 corresponds to f = 0.5), and t_i is the time in days between the sampling date and any previous monthly rain (i).

4.0 Results and Discussion

Water column ^{7}Be activities are presented in Supplemental Table 1. The ^{7}Be inventories are shown in Table 1 and plotted against latitude with the weighted average rainfall rates (Eqn. 4) in Figure 2a. The gradients in the climatological rain rates from Figure 1 are reflected in those of the cruise with the peak in rainfall corresponding to the Intertropical Convergence Zone (ITCZ). Generally the ^{7}Be inventories follow the trend in rainfall, the exception occurring at the zone of equatorial upwelling. There, the observed ^{7}Be inventory does not reflect atmospheric input, but rather upwelling of deep, ^{7}Be-deficient water. This observation has been used to derive upwelling rates (Kadko and Johns, 2011; Haskell et al., 2014; Kadko, 2017). In Figure 2b, the ^{7}Be inventories are plotted against rain rate. The two parameters are correlated, with higher inventories occurring within zones of high rainfall. The ^{7}Be inventories at upwelling stations fall well below the trendline.

Table 1. ^{7}Be Data from the PMT (GP15) cruise

Water column ^{7}Be inventories			**Aerosol ^{7}Be Activities**		
station	Lat (^{0}N)	^{7}Be Inventory (dpm/m^{2})	Aerosol Deployment	Latitude (sample midpoint)	^{7}Be Activity (dpm/m^{3})
4	54.66	23390	3	54.9	0.0184±0.0066
5	53.68	21520	4	53.3	0.0366±0.0015
6	52.0	24750	1	49.5	0.0622±0.0094
8	47.0	25460	5	51.1	0.1567±0.0054
10	42.0	22580	6	45.75	0.2660±0.0079
12	37.0	22470	7	43.25	0.2935±0.0089
14	32.0	22460	8	39.5	0.1232±0.0053
16	27.0	19980	9	35.75	0.2730±0.0076
18	22.0	15860	10	33.25	0.1818±0.0073
19	17.5	21900	11	29.5	0.2770±0.0083
21	11.0	18240	12	24.5	0.1754±0.0075
23	7.5	29830	13	18.1	0.0975±0.0106
25	5.0	28880	14	14.25	0.0792±0.0084
27	2.5	15550	15	8.8	0.0413±0.0046
29	0	4015	16	5.725	0.0984±0.0059
31	-2.5	8020	17	3.45	0.1848±0.0079
33	-5.0	1730	18	0.415	0.1373±0.0053
35	-10.5	16640	19	-3.1	0.1222±0.0105
37	-15	21610	20	-7.75	0.1492±0.0074
39	-20	23320	21	-12.75	0.1080±0.0076
			22	-17.5	0.1482±0.0066
			23	-19.6	0.2147±0.0133

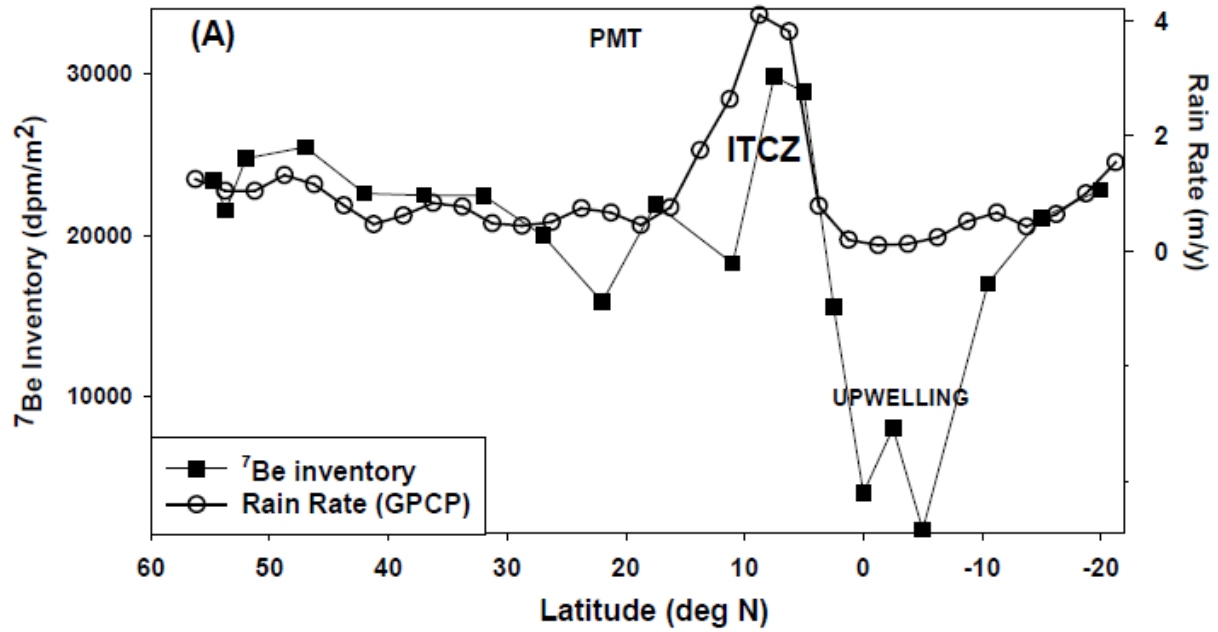

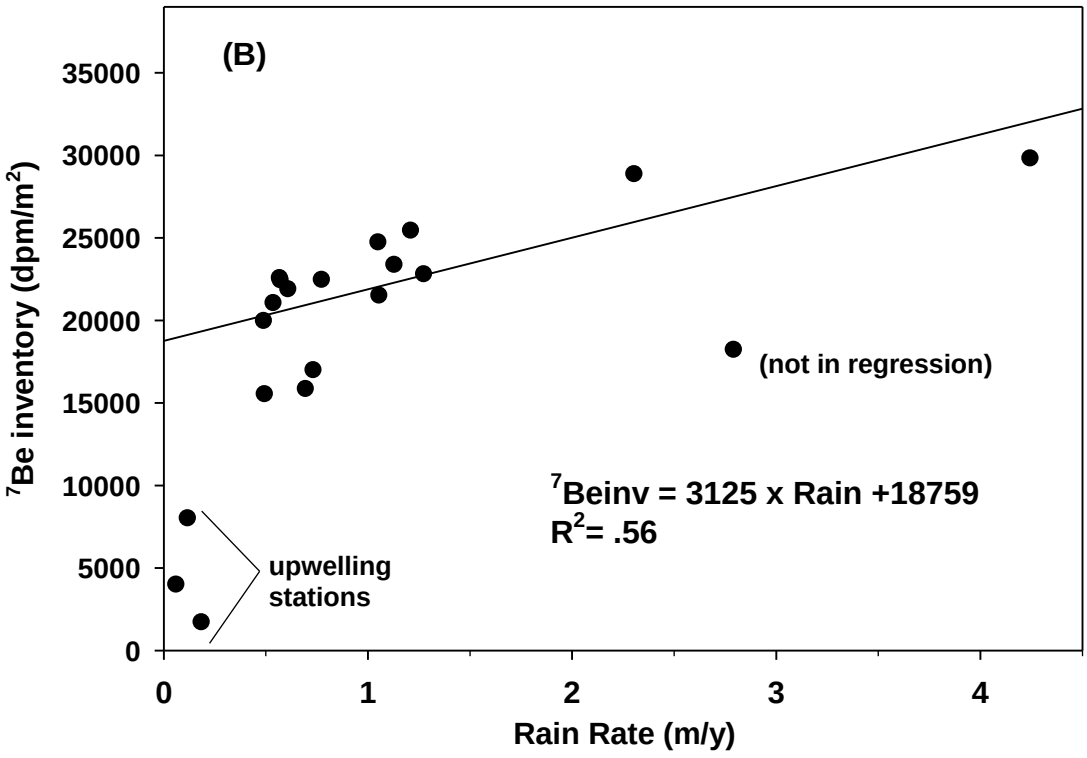

Figure 2. (A) The ^{7}Be inventories (squares) and the weighted average rain rate (circles) plotted against latitude for the PMT transect. The locations of the ITCZ and upwelling region are indicated. (B) The ^{7}Be inventories plotted against rain rate. The upwelling stations fall well below the trendline.

The ^{7}Be aerosol activities are shown in Table 1 and plotted against latitude with the weighted average rain rate (Eqn. 4) in Figure 3a. There is no obvious relationship between the ^{7}Be aerosol activities and the rain rate with the exception of aerosols collected within the ITCZ. There the persistent high rainfall maintains a low aerosol ^{7}Be activity (e.g. Feely et al, 1989). This is shown in Figure 3b, where in a plot of ^{7}Be aerosol concentration against rain rate the ITCZ samples represent a separate relationship from the other samples. The average ^{7}Be aerosol activity of the three ITCZ samples is 0.073 ± 0.029 dpm/m^{3}, and that for the other 19 samples is 0.157 ± 0.075 dpm/m^{3}.

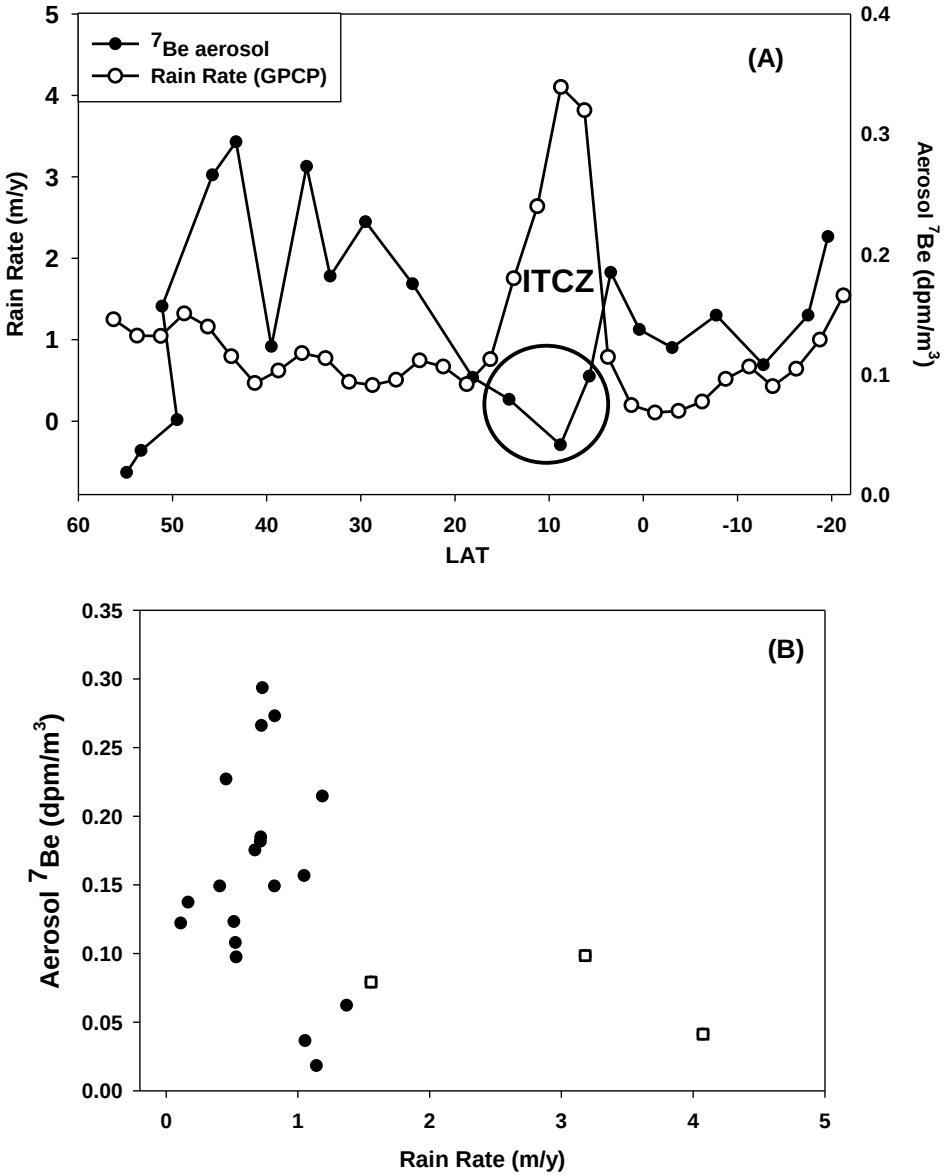

Figure 3. (A) The ^{7}Be aerosol activities (black circles) and weighted average rain rate (open circles) plotted against latitude for the PMT cruise track. The location of the ITCZ is indicated and aerosol samples collected within the ITCZ are circled. (B) The ^{7}Be aerosol activities plotted against rain rate. The aerosol samples collected within the ITCZ are indicated (open squares).

To derive the bulk deposition velocities (V_b), the ^{7}Be inventories (Table 1) are combined with the aerosol ^{7}Be activities (Eqn. 3; Table 1). The ^{7}Be inventories integrate deposition over the mean life (77 days) of the isotope, and the rain rate is based on monthly averages. However, each aerosol sample is collected over a period of only several days, and atmospheric transport is temporally and spatially sporadic such that variability in aerosol ^{7}Be activity rather than variability in the upper ocean inventory would drive variability in V_b. For this reason we use an average aerosol ^{7}Be activity rather than the "snapshot" aerosol observations to calculate the bulk deposition velocities. Values of V_b derived in this manner for the PMT cruise are plotted against rain rate in Figure 4. Across the PMT transect V_b and rainfall are well correlated (R^2=0.81), and the results from Bermuda and the Arctic Ocean (Kadko et al., 2015; Kadko et al., 2016; 2019) fall on the PMT trendline.

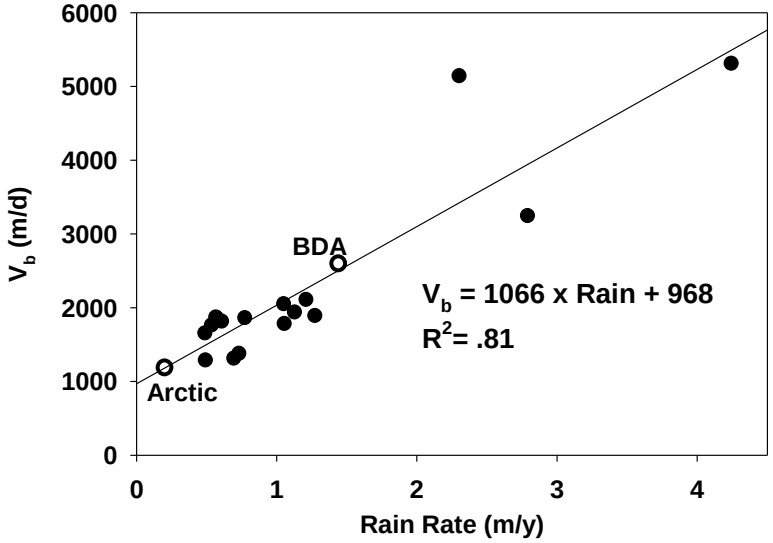

Figure 4. The bulk deposition velocity (V_b) plotted against rain rate for the PMT transect (black symbols). The Bermuda and Arctic results are shown for comparison.

The ^{7}Be inventories from this work (PMT) are plotted with those from several earlier studies, against rainfall in Figure 5a. The general trend of increasing inventory with rainfall is observed. Dividing these data by the approriate aerosol ^{7}Be concentrations yields a set of V_b values that are plotted against rain rate in Figure 5b. A high correlation between V_b and rain rate is observed across several ocean basins. Scatter in the inventory plot (Fig 5a) is reduced in Figure 5b as high inventories (e.g. Bermuda), are driven by high aerosol concentration, while low inventories (e.g. Arctic) are driven by low aerosol concentrations. The resulting relationship is

$$V_b \text{ (m/d)} = 999 \pm 96 \text{ x RainRate} + 1040 \pm 136 \qquad \text{Eqn. 5}$$

The y- intercept indicates a dry deposition velocity of 1040 m/d.

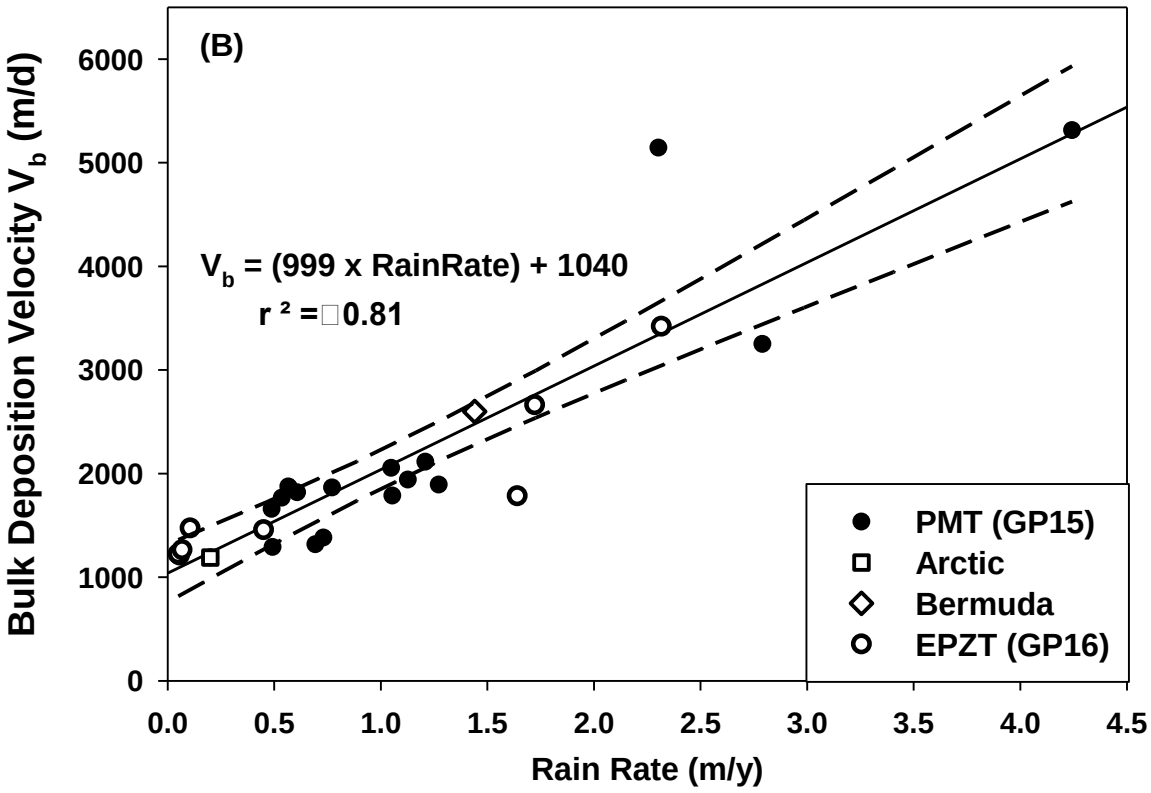

Figure 5 (A). The ^{7}Be inventories plotted against rain rate for the PMT cruise (black circles); the EPZT (open circles, Kadko et al., in review); Bermuda (diamond, Kadko et al.; 2015) and the Arctic (square, Kadko et al., 2016; 2019). B) V_b plotted against rain rate for these same locations. The upper and lower 95% confidence intervals (dashed lines) around the linear regression trend line are shown.

5.0 Conclusions

In this work, ocean ^{7}Be inventories and aerosol ^{7}Be concentrations collected during the GEOTRACES Pacific Meridional Transect were used with data from other ocean basins to derive a global relationship between rainfall rate (m/y) and aerosol bulk deposition velocity (m/d), where V_b = 999±96 x Rain rate + 1040±136 (R^2=0.81). Future work can further test whether the bulk deposition velocities derived using this relationship, based on aerosol ^{7}Be, can be used to reliably calculate the fluxes of other TEs. This has been tested at Bermuda and the Arctic with good success. With this relationship, the fluxes of soluble aerosol bioactive elements to the surface ocean can be calculated by multiplying the aerosol bulk deposition velocities times the aerosol TE concentrations and solubilities, (e.g. Buck et al., 2019; Kadko et al., 2019). This information is critical for evaluating limitations on phytoplankton growth and the strength of the Biological Carbon Pump, and represents an important constraint on ocean biogeochemical models.

Acknoweldgements

This work was upported by NSF grants OCE-1736319 to DK, OCE-1756104 to WML, and OCE-1756103to CSB. Data have been submitted to the Biological and Chemical Oceanography Data Management Office (BCO-DMO) (https://www.bco-dmo.org/dataset/781794 and https://www.bco-dmo.org/dataset/781806) and will appear in future GEOTRACES data products. We thank Drs. Mark Stephens and Chris Marsay for their technical assistance.

References

Anderson, R. F., H. Cheng, R. L. Edwards, M. Q. Fleisher, C. T. Hayes, K.-F. Huang, D. Kadko, P. J. Lam, W. M. Landing, Y. Lao, Y. Lu, C. I. Measures, P. L. Morton, S. B. Moran, D. C. Ohnemus, L. F. Robinson, R. U. Shelley (alphabetical order) (2016), How well can we quantify dust deposition to the ocean? Philosophical Transactions of the Royal Society A 374, DOI: 10.1098/rsta.2015.0285.

Baker, A.R. and T.D. Jickells. (2016). Atmospheric deposition of soluble trace elements along the Atlantic Meridional Transect (AMT). Prog. Oceanogr. doi:10.1016/j.pocean.2016.10. 002.

Baker A. R., Landing W. M., Bucciarelli E., Cheize M., Fietz S., Hayes C. T., Kadko D., Morton P. L., Rogan N., Sarthou G., Shelley R. U., Shi Z., Shiller A. and van Hulten M. M. P. (2016). Trace element and isotope deposition across the air–sea interface: progress and research needs. Philosophical Transactions of the Royal Society A: Mathematical, Physical and Engineering Sciences. http://doi.org/10.1098/rsta.2016.0190.

Buck., C.S., A. Aguilar-Islas, C. Marsay, D. Kadko and W. Landing (2019) Trace element concentrations, elemental ratios, and enrichment factors observed in aerosol samples collected during the US GEOTRACES eastern Pacific Ocean transect (GP16). Chem. Geo., 511, 212-224.

Coale K.H., K.S. Johnson, S.E. Fitzwater, R. M. Gordon, S. Tanner, F. P. Chavez, L. Ferioli, C. Sakamoto, P. Rogers, F. Millero, P. Steinberg, P. Nightingale, D. Cooper, W. P. Cochlan, M. R. Landry, J.Constantinou, G. Rollwagen, Trasvina A. and R. Kudela. (1996) A massive phytoplankton bloom induced by an ecosystem-scale iron fertilization experiment in the equatorial Pacific Ocean. Nature 383, 495 - 501; doi:10.1038/3834

Duce, R.A., P. S. Liss J. T. Merrill E. L. Atlas P. Buat, Menard B. B. Hicks J. M. Miller J. M. Prospero R. Arimoto T. M. Church W. Ellis J. N. Galloway L. Hansen T. D. Jickells A. H. Knap K. H. Reinhardt B. Schneider A. Soudine J. J. Tokos S. Tsunogai R. Wollast M. Zhou. (1991). The atmospheric input of trace species to the world ocean. Global Biogeochem. Cycles 5, 193-259, doi:10.1029/91GB01778.

Falkowski, P. (1997) Evolution of the nitrogen cycle and its influence on the biological sequestration of CO2 in the ocean, Nature 387, 272 - 275, doi:10.1038/387272a0.

Falkowski, P.G., R.T. Barber, and V. Smetacek (1998) Biogeochemical controlsand feedbacks on ocean primary production. Science 281, 200-206.

Feely, H.W., R. J. Larsen & C, G. Sanderson (1989) Factors That Cause Seasonal Variations in Beryllium-7 Concentrations in Surface Air. I. Environ. Radioactivity 9, 223-249

Haskell W.Z., D. Kadko, D.E. Hammond, M.G. Prokopenko, W.M. Berelson, A.N. Knapp and D. Capone (2015) Upwelling velocities and eddy diffusivity from 7Be measurements used to compare vertical nutrient fluxes to export POC flux in the Eastern Tropical South Pacific. Marine Chemistry. doi:10.1016/j.marchem.2014.10.004. 168, 140–150.

Jickells, T.D., P. Boyd, K.A. Hunter. (2014). Biogeochemical impacts of dust on the global carbon cycle. In: Knippertz, P., Struut, J.-B.W. (Eds.), Mineral Dust. Springer Heidelberg

Kadko, D., and J. Prospero (2011), Deposition of 7Be to Bermuda and the regional ocean: Environmental factors affecting estimates of atmospheric flux to the ocean, J. Geophys. Res., 116, C02013, doi:10.1029/2010JC006629.

Kadko, D., and W. Johns (2011) Inferring upwelling rates in the equatorial Atlantic using 7Be measurements in the upper ocean. Deep-Sea Res. I, 58, 247-257, doi:10.1016/j.dsr.2011.03.004

Kadko D., W. M. Landing, and R. U. Shelley (2015) A novel tracer technique to quantify the atmospheric flux of trace elements to remote ocean regions. Journ. Geophy. Res. Oceans, 119, doi:10.1002/2014JC010314.

Kadko D., B. Galfond, W. M. Landing, and R. U. Shelley (2016) Determining the Pathways, Fate, and Flux of Atmospherically Derived Trace Elements in the Arctic Ocean/Ice System. Marine Chemistry. 182, 38-50, doi:10.1016/j.marchem.2016.04.006.

Kadko, D. (2017) Upwelling and Primary Production during the U.S. GEOTRACES East Pacific Zonal Transect. Global Biogeochem. Cycles. 31, doi:10.1002/2016GB005554.

Kadko D., A. Aguilar-Islas, C. Bolt, C.S. Buck, J. N. Fitzsimmons, L. T. Jensen, W.M. Landing, C.M. Marsay, R. Rember, A. M. Shiller, L. M. Whitmore, and R. F. Anderson (2019) The residence times of trace elements determined in the surface Arctic Ocean during the 2015 US Arctic GEOTRACES expedition. Mar. Chem. 208, 56-69. doi.org /10.1016/ j.marchem. 2018.10.011.

Kadko, D., A. Aguilar-Islas, C. S. Buck, J. N. Fitzsimmons, W. M. Landing, A. Shiller, C.P. Till, K.W. Bruland, E.A. Boyle, R.F. Anderson (in review) Sources, Fluxes and Residence Times of Trace Elements measured during the U.S. GEOTRACES East Pacific Zonal Transect. Mar Chem.

Kim, G., L. Alleman, and T. Church (1999) Atmospheric depositional fluxes of trace elements, ^{210}Pb and ^{7}Be into the Sargasso Sea. Global Biogeochem. Cycles, 13, 1183-1192.

Krishnamurthy A., J.K. Moore, N. Mahowald, C. Luo, S.C. Doney, K. Lindsay and C. S. Zender. (2009). Impacts of increasing anthropogenic soluble iron and nitrogen deposition on ocean biogeochemistry. Global Biogeochemical Cycles, 23, doi:10.1029/2008GB003440.

Mahowald, N. M., A. R. Baker, G. Bergametti, N. Brooks, R. A. Duce, T. D. Jickells, N. Kubilay, J. M. Prospero, and I. Tegen (2005), Atmospheric global dust cycle and iron inputs to the ocean, Global Biogeochem. Cycles,19, GB4025,doi:10.1029/2004GB002402.

Marsay, C.M., D. Kadko, W. M. Landing, P. L. Morton, B.A. Summers and C. S. Buck (2018) Concentrations, provenance and flux of aerosol trace elements during US GEOTRACES Western Arctic cruise GN01, Chem. Geol., 502, 1-14.

Martin, J.H., S. E. Fitzwater and R. M. Gordon. (1990). Iron deficiency limits phytoplankton growth in Antarctic waters, Global Biogeochem. Cycl., 4: 5-12.

Moore, C.M., et al. 2009 Large-scale distribution of Atlantic nitrogen fixation controlled by iron availability. *Nature Geoscience* **2**, 867-871.

Moore, C.M., et al. 2013 Processes and patterns of oceanic nutrient limitation. *Nature Geoscience* **6**, 701-710.

Moore, J.K., S.C. Doney, D.M. Glover, and I.Y. Fung 2002 Iron cycling and nutrient-limitation patterns in surface waters of the World Ocean. *Deep-Sea Research Part II-Topical Studies in Oceanography* **49**, 463-507.

Morel, F.M.M. and Price, N.M. (2003). The biogeochemical cycles of trace metals in the oceans. Science, 300: 944-947.

Morel, F.M.M., Milligan, A.J. and Saito, M.A., (2003). Marine bioinorganic chemistry: The role of trace metals in the oceanic cycles of major nutrients. In The Oceans and Marine Geochemistry. Treatise on Geochemistry (ed. H. Elderfield), pp. 113-143.Oxford: Elsevier.

Okin, G.S., et al. 2011 Impacts of atmospheric nutrient deposition on marine productivity: Roles of nitrogen, phosphorus, and iron. *Global Biogeochemical Cycles* **25**.

Olsen, C.R., Larsen, I.L., Lowry, P.D., Cutshall, N.H., Todd, J.F., (1985). Atmospheric fluxes and marsh-soil inventories of 7Be and 210Pb. J. Geophys. Res. 90 (10), 487–495.

Peng, A., G. Liu, Z. Jiang, G. Liu, M. Liu (2019) Wet depositional fluxes of 7Be and 210Pb and their influencing factors at two characteristic cities of China. Applied Radiation and Isotopes, 147, 21-30.

Prospero J.M. (1996) Saharan Dust Transport Over the North Atlantic Ocean and Mediterranean: An Overview. In: Guerzoni S., Chester R. (eds) The Impact of Desert Dust Across the Mediterranean. Environmental Science and Technology Library, vol 11. Springer, Dordrecht.

Prospero J.M. (2002) The Chemical and Physical Properties of Marine Aerosols: An Introduction. In: Gianguzza A., Pelizzetti E., Sammartano S. (eds) Chemistry of Marine Water and Sediments. Environmental Science. Springer, Berlin, Heidelberg.

Schanze, J.J., R. W. Schmitt, and L. L. Yu (2010) The global oceanic freshwater cycle: A state-of-the-art quantification. Journal of Marine Research, 68, 569–595.

Shelley, R.U., M. Roca-Martí, M.Castrillejo, V. Sanial, P. Masqué., W. M. Landing, P. van Beek, H. Planquette, G. Sarthou (2017) Quantification of trace element atmospheric deposition fluxes to the Atlantic Ocean (> 40°N; GEOVIDE, GEOTRACES GA01) during spring 2014.

Tagliabue, A., L. Bopp, O. Aumont (2009) Evaluating the importance of atmospheric and sedimentary iron sources to Southern Ocean biogeochemistry. GEOPHYSICAL RES. LET. 36, L13601, doi:10.1029/2009GL038914.

Tagliabue, A., O. Aumont, R. DeAth, J. P. Dunne, Stephanie Dutkiewicz, E. Galbraith, K. Misumi, J K. Moore, A. Ridgwell, E. Sherman, C. Stock, M. Vichi, C.Völker, Andrew Yool (2015) How well do global ocean biogeochemistry models simulate dissolved iron distributions? Global Biogeochem. Cycles,30, 149–174,doi:10.1002/2015GB005289.

Uematsu, M., R. A. Duce and J. M. Prospero (1994) Atmosphere beryllium-7 concentrations over the Pacific Ocean. Geophy. Res. Lett. 21, 561-564.

Volk, T. and Hoffert, M.I. (1985) Ocean carbon pumps: Analysis of relative strengths and efficiencies in ocean-driven atmospheric CO2 changes, in: Sundquist, E.T., Broecker, W.S. (Eds.), The Carbon Cycle and Atmospheric CO2: Natural Variations Archean to Present. American Geophysical Union, Washington, D. C., pp. 99-110.

Young, J. A., and W. B. Silker (1980), Aerosol deposition velocities on the Pacific and Atlanic Oceans calculated from 7Be measurements, Earth Planet. Sci. Lett., 50, 92–104, doi:10.1016/ 0012-821X(80)90121-1.